



Support-Free-Material Path Generation for DED Processes from Facetized Data

Lewis Andurand, Vincent Hugel, Sébastien Campocasso, Matthieu Museau

► To cite this version:

Lewis Andurand, Vincent Hugel, Sébastien Campocasso, Matthieu Museau. Support-Free-Material Path Generation for DED Processes from Facetized Data. 16th CIRP Conference on Intelligent Computation in Manufacturing Engineering (CIRP ICME), Jul 2022, Online, Italy. pp.632-637, 10.1016/j.procir.2023.06.108 . hal-04197344

HAL Id: hal-04197344

<https://hal.science/hal-04197344>

Submitted on 7 Sep 2023

HAL is a multi-disciplinary open access archive for the deposit and dissemination of scientific research documents, whether they are published or not. The documents may come from teaching and research institutions in France or abroad, or from public or private research centers.

L'archive ouverte pluridisciplinaire **HAL**, est destinée au dépôt et à la diffusion de documents scientifiques de niveau recherche, publiés ou non, émanant des établissements d'enseignement et de recherche français ou étrangers, des laboratoires publics ou privés.

Support-Free-Material Path Generation for DED Processes from Facetized Data

Lewis Andurand^{a,*}, Vincent Hugel^a, Sébastien Campocasso^a, Matthieu Museau^b

^aToulon University, Avenue de l'Université, 83130 La Garde, France

^bGrenoble-Alpes University, 46 Avenue Félix Viallet, 38000 Grenoble, France

* Corresponding author. E-mail address: lewis-andurand@etud.univ-tln.fr

Abstract

Directed Energy Deposition (DED) processes are a category of Additive Manufacturing (AM) processes that can be combined with six degrees of freedom multi-axis technologies to manufacture parts with complex internal geometries without support material, while ensuring the local distance requirements. This paper provides a numerical method to compute such a path, using both a facetized file of a part and substrates locations as inputs. Topological concepts are first described to introduce the method. The algorithm is then detailed into three steps: mesh refinement, next layer points search and connection edges computing. Application to different facetized files validates the method.

© 2022 The Authors. Published by Elsevier B.V.

Peer-review under responsibility of the scientific committee of the 16th CIRP Conference on Intelligent Computation in Manufacturing Engineering.

Keywords: Path generation, Additive Manufacturing, Directed Energy Deposition, Triply-periodic minimal surfaces

1. Introduction

Directed Energy Deposition (DED) is a category of Additive Manufacturing (AM) processes in which parts are formed by deposition of successive layers of melting material [1]. Heat input and material feeding are paired in DED technologies. This feature makes them easier to combine with multi-axis robots. For this, such processes have been considered to be serious candidates for the manufacturing of complex parts that cannot be obtained with subtractive technologies [2]. In particular, this is the case of mechanical parts filled with inner structures. The filling of parts with optimized inner structures leads to the increase of mechanical performances (mainly, mechanical strength and elasticity) or a reduction of mass for equivalent mechanical properties [3]. Optimized structures can have complex shapes and thus require a complex deposition tool trajectory.

Among all DED processes, Wire and Arc Additive Manufacturing (WAAM) was shown as a promising solution for the manufacturing of metallic parts in terms of cost per unit [4]. Some studies over the last 15 years have highlighted that

the control of the distance between the tool and the workpiece is one of the necessary parameters to deal with the energy input of the arc and thus local deposition [5]. Thus; keeping a constant distance between the tool and the workpiece during the manufacturing process helps to maintain the constancy of the metallic microstructure all over the part [6]. The use of a constant Euclidean distance between the tool and the workpiece is a constraint that can also be used on other DED processes to ensure that the material is always close enough to the workpiece and thus prevent the deposit material from collapsing during the manufacturing process. Consequently, this distance constraint leads to manufacturing paths that do not necessarily require the use of support-material.

Traditional AM path computing techniques involve the use of slicers to create Z-level layers but this does not guarantee that the Euclidean distance criterion is met. This also requires the adding of support material to prevent part collapsing during the manufacturing process. Some techniques were developed over the last 5 years to solve this and compute the path of some basic surfaces [7,8]. The paths computed differ from the ones obtained with a basic slicing and meet the distance criterion.

However, the algorithms developed are shape-specific and cannot be adapted to complex paths. In addition, such methods require the use of a bi-parametric equation of the surface to manufacture, which does not necessary exist for any pattern-filled mechanical part.

This paper presents a generic numerical method to compute the deposition path of any surface stored in a facetized format given any substrate location. The path computed does not require the use of support material and minimizes the number of deposition layers. For this, some topological concepts are first introduced. Then, the main steps of the algorithm, from points computing to path points ordering, are presented and illustrated with the case of the Schwarz Primitive (Schwarz P) surface, which is a Triply Periodic Minimal Surface (TPMS). The algorithm is also applied to two other TPMS to validate the versatility of the method: the Schwarz Gyroid (Schwarz G) surface and the Neovius surface.

The nomenclature below sums up the main input parameters of the path generation algorithm.

Nomenclature	
h	inter-layer distance
e	mesh faces edges maximum length
d	layers discretization indicative value
f	minimum distance between graphs non-connex nodes

2. Topological concepts

Path generation for DED processes consists in finding the next layer of the path, given the previous one. The approach is iterative. A layer is defined as a set of points and edges between these points. In order to satisfy the constant Euclidean distance between the tool and the workpiece, each point of the layer under computing must be at a distance h from the set of edges and points of the workpiece. In the particular case of path generation with number of layers minimization, this corresponds to the distance between the points of the current layer under computing and the previous layer. The path between two successive nodes is interpolated by a line, which is a valid approximation, provided that the layer discretization value d is small enough for the inter-layer distance h , since h can also be seen as the limit of accuracy of detail of the manufactured part. In case d tends to 0, the layer under computing tends to the ideal layer of the path so that it is away from the previous layer by a distance of h at every location.

This property is reminiscent of the idea of contour lines in geography, that correspond to lines of constant elevation or depth. More specifically, the construction of layers reminds the concept of iso-geodesic lines on surfaces. The use of geodesics was one of the first approach used to compute paths for AM processes [9]. By applying a flow propagation over the surface from a source point and by solving the transport equation, one can find all the iso-minimal-arc-length (iso-MAL) curves on the surface of this source point. Many physical phenomena are governed by flow propagation, such as heat propagation, and

waves propagation in continuous and homogeneous fields. With this approach, the next layer of the path is obtained by finding the iso-MAL curves of arc length h from a set of source points located at every point of the previous layer of the path. However, such distances are length of curves lying on the surface (Fig. 1-a), which means that the distances depend on the local variations of the curvature of the surface along the curve. This does not necessary guarantee that the end points of the iso-MAL curve are distant of a constant Euclidean length (Fig. 1-b). In particular, this is especially significant for high curvature variation surfaces because the length of the iso-MAL curve between two points and is cumulative and depends on the shape of the surface whereas the Euclidean distance only depends on the coordinates of these point, and thus does not depend on the geometry of the support surface.

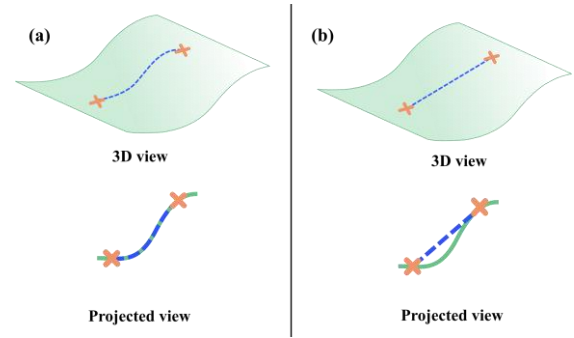


Fig. 1. (a) Geodesic distance; (b) Euclidean distance

As a result, the use of iso-MAL curves is restricted to surfaces with low curvature variations. However, the surface of the patterns used to fill lightened mechanical parts can be complex. In particular, this is the case of TPMS [3] where a method which is directly adapted to Euclidean distances is relevant and may lead to different layers than the ones obtained with the iso-MAL curves.

As explained, Euclidean distances are characterized by two properties:

1. Only points coordinates are required to compute the relative distance between points.
2. Euclidean distances are not cumulative.

The direct consequence of point 1 is that the data of the surface to manufacture must contain coordinates information. The most common 3D surface objects formats are Stereolithography (STL), 3D Object (OBJ), Initial Graphic Exchange Specification (IGES) and Standard for Exchange of Product Data (STEP) (Table 1.). For this, a discretized input format of surface data is more relevant than a parametric input format. The STL format was chosen to develop the algorithm because of the simplicity and unicity of the objects structure. The unicity of structure objects makes the algorithm less case-specific. All faces are triangles, which makes the computing of faces simpler. In counterpart, STL files have a lower accuracy than OBJ ones, leading to more voluminous files for a same accuracy of surface details.

Table 1. Common Surface Data Numerical Formats Comparison

Abbreviation	Data type	Structure of objects	Accuracy
STL	Discretized	Triangular faces	Quite low
OBJ	Discretized	Polygonal faces	Medium
IGES	Parametric	Curves, curved surfaces	Quite high
STEP	Parametric	Curves, curved surfaces	High

The consequence of point 2 is that each layer depends on its previous layer. Consequently, all layers should be computed successively. If the distances were cumulative, such as for isothermal curves, any layer of the path could be computed given only one layer of the path.

3. Path generation algorithm

The aim of the path generation algorithm is providing the sequence of tool positions and orientations for the manufacturing process. Each point has to meet the Euclidean distance criterion h to ensure there is always workpiece material to support the melting material being deposited. All points are connected by edges. In addition, the computed edges have to be ordered to minimize deposition starts and stops.

The algorithm of path generation has four steps. The first one consists in mesh subdivision. The second one is substrates zones declaration to build the initialization layer of the path. The points of the next layer are computed during the third step. Lastly, the next layer points are organized into a graph to connect all deposition points with edges. The third and fourth steps are repeated until there are no more layers to compute.

3.1. Mesh subdivision

The input format of the 3D surface data used in the algorithm is STL. The geometry of triangles is well known and has been used over the years for several computing techniques: computer 3D rendering, collision detection, and fast prototyping. This is also the common format for 3D printing, and is widely used in Computer Aided Design (CAD) software. The format describes the external surface of a closed volumetric 3D object. It fully describes 3D surfaces. The entire surface is split into a set of triangles connected by their edges and vertices. This splitting is called “tessellation” and the whole set of triangular faces is called “mesh”. Each triangular face is described by the Cartesian coordinates (x,y,z) of its three vertices, and the unit vector normal to the plane of the triangle and oriented toward the exterior of the surface in case the 3D object is a closed volume. The orientation of the normal vector is arbitrary for a 3D surface because there is no distinction between the interior and the exterior.

The 3D surface tessellation of STL protocol creates all the triangular faces of the mesh. The mesh tessellation is not unique. The number, size and angles of mesh is governed by input parameters: maximum faces edges length, possibly minimum triangle angles, and precision requirement to fit the ideal surface the tessellation is created from. One of the most common algorithms used to create a tessellation is Delaunay triangulation.

Mesh processing before path computing consists in two successive steps: initial mesh refinement and faces associated graph creation (Fig. 2). During the computing process of a new layer of the trajectory, the mesh is used to find points distant of h from the previous layer. This requires to use all the mesh data for each point computing.

In order to reduce the computing time, the mesh faces used are removed from the remaining mesh used for path calculation. This implies that triangular faces edges are small enough compared to h . For this, the initial mesh is subdivided into a smaller mesh with new triangles whose edges are smaller than a limit value e . The limit e is the input parameter of mesh refinement and has to be smaller than h to ensure that no triangular face is common to two different layers and hence can be removed from the remaining mesh during computing. Each triangle is split into smaller triangles. Splitting one triangle consists in the adding of one vertex on the longer edge and the adding of the edge linking this new vertex and the vertex of the mother triangle opposed to the longer edge. The location of the new vertex depends on the geometry of the mother triangle, and each child triangle can be split into two smaller triangles again depending on its size. This approach guarantees that children faces are triangles too. However, these new triangles are not necessarily connected.

Mesh connection is not required to compute the path, but all faces connexion neighbourhood information is needed to avoid to create edges between points of the layer under computing that are not supposed to be connected. This is in particular required for complex 3D surfaces with holes and folds. Consequently, a graph is built from the initial connected mesh using the common vertices. Then, each initial triangular face is associated to a connexion index. In case of a connex 3D part, all triangles have the same connexion index. Lastly, all children faces inherits graph information (graph node index and connexion index) from their initial mother face.

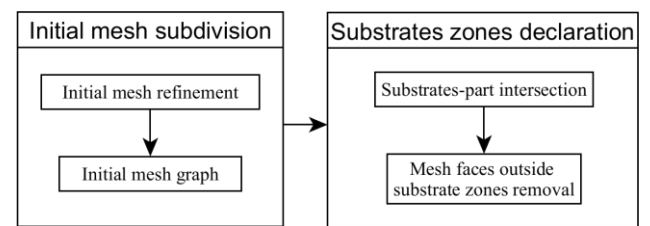


Fig. 2. Path generation steps 1 and 2 flowcharts.

3.2. Substrates zones declaration and initialization layer

Each new layer of the path is created from its previous layer. Consequently, an initialization layer is necessary to compute the first layer and trigger the spreading of the successive layers. This initialization layer is defined as the intersection of the substrate and the part to manufacture. Hence, the knowledge of the substrates associated to the surface to build is required for trajectory initialization. In the case of the Schwarz P, the substrate is a plane (Fig. 3).

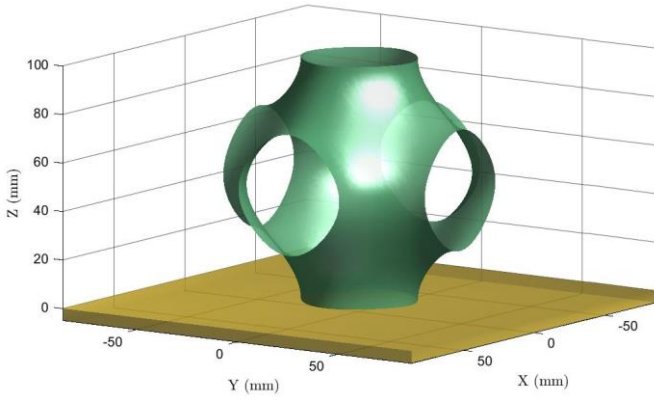


Fig. 3. Schwarz P surface (green) and its substrate (yellow).

This initialization layer lies both on the surface of the substrate and the part to manufacture. Therefore, this layer is defined as the intersection between the substrates and the part (Fig. 4). The substrates zones are imported as closed volumetric 3D objects of STL format. This intersection is computed using a mesh-mesh intersection algorithm adapted from ray-triangle intersection techniques used in computer 3D rendering. The intersection is stored as a set of edges.

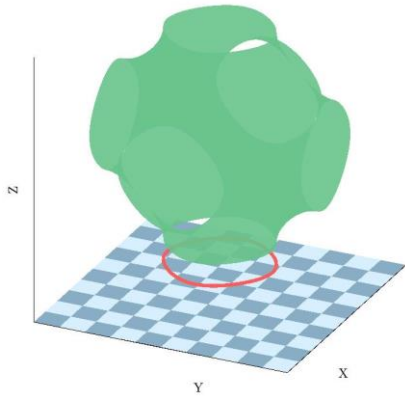


Fig. 4. Schwarz P path initialization layer (red).

Lastly, the set of edges of the initialization layer is sorted to create a path way of the intersection curve. This ordered path is computed by associating the set of edges to a graph. An algorithm inspired from the Chinese Postman Problem (CPP) of the graph theory is applied [10]. The output ordered path minimizes the displacements to visit all the edges of the intersection curve. Although the path of initialization layer is not followed by the deposition tool, its ordering makes the construction of the tool ordered path of the first layer easier. Then, edges of the graph are subdivided into smaller edges so that no edge length is greater than the discretization value d .

3.3. New layer points computing

At this stage of the algorithm, a previous ordered layer is supposed to exist. If the next layer is the first layer of the path,

the previous layer is the initialization layer. As explained in the introduction of this paper, the path generation algorithm minimizes the number of layers. Consequently, there is no more layer to compute if the previous layer computed is empty. In that case, the path generation is completed.

The generation of the new layer is based on three stages applied for each point of the previous layer: triangle-sphere intersections, computing of spherical linear interpolations (SLERP) and circle arcs merging (Fig. 6).

During the first stage, the intersections between several spheres and the remaining mesh are computed (Fig. 5-a). The spheres are centred on the points located on the previous layer, and the radius is the inter-layer distance h . The spheres are used consecutively in accordance with their centre position on the graph of the previous layer. For each point, the remaining mesh triangular faces that intersect the associated sphere are detected. The intersection existence is determined by the method of separating axis [11] adapted to the case of a sphere. This method is a generic approach for collision detection that has application in robotics and real time 3D graphics rendering. It determines if a point collides a volumetric closed convex 3D surface. When modified to fit with the path generation problem, it detects which faces of the triangular faces of the mesh collide the sphere. The faces located inside the sphere are deleted from the remaining mesh, and the faces that intersect the surface of the sphere are kept for the second stage.

The second stage is SLERP computing. For each triangle concerned, the type of intersection is a set of arcs circles from a same circle, from one to three arcs depending on the type of intersection. Limit cases with circle arcs equivalent to a single point are not considered. The circle arcs end points lie on the edges of the triangle. Then, each circle is discretized and ordered as a subgraph by applying a SLERP [12] to the vectors \vec{u} and \vec{v} starting from the centre of the sphere and pointing respectively to the start point and the end point of the circle arc (Fig. 5-b).

Finally, the circle arcs are merged during the third stage. The subgraphs of circle arcs having a common end point are merged into a single connected subgraph. At the end of the three stages, a set of organized subgraphs of the next layer is obtained.

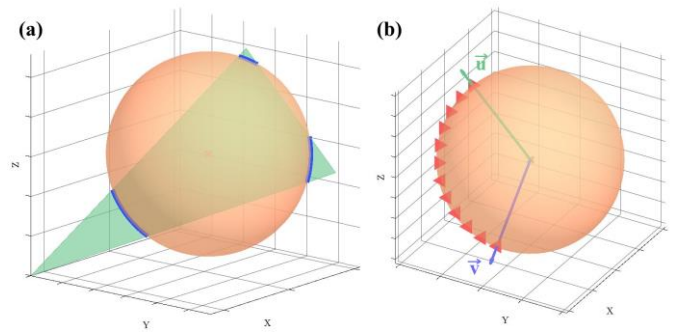


Fig. 5. (a) Triangle-sphere intersections (blue); (b) SLERP (red).

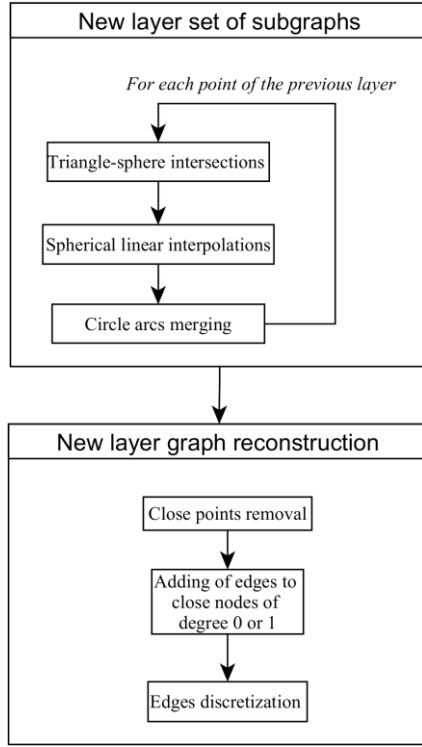


Fig. 6. Path generation steps 3 and 4 flowcharts.

3.4. New layer graph reconstruction

The set of organized subgraphs is part of the ordered path of the next layer. To obtain the full graph of the new layer, edges are added to connect the subgraphs. Each set of subgraphs associated to a same sphere do not require any adding of edges, due to the circle arcs merging stage. However, subgraphs associated to different spheres have to be connected if necessary. The new layer graph reconstruction consists in three tasks: close points removal, adding of edges to close nodes of different graphs, and edges discretization (Fig. 6). Then, a path way is computed with respect to the CPP.

First, points of two different subgraphs close to less than a certain distance are filtered. The filtering distance f is supposed to be smaller than the distance of discretization d . Given two points of two different subgraphs close to less than a distance f , the one from the subgraph with the lowest number of nodes is removed from the next layer data. All the edges connected to this deleted node are also removed. This can lead to an increase of the number of subgraphs because each subgraph with a deleted node can become unconnected. All the children subgraphs are the connected components of the mother subgraphs.

After the filtering task, edges are added to connect properly the subgraphs. To this end, edges are added between nodes of two different subgraphs. The degree of a node corresponds to the number of edges directly connected to this node. Only the nodes of degree 0 or 1 are considered during this process. Two nodes are connected if they are close to a distance less than $e+f$. Because e corresponds to the maximal length of the triangles of the subdivided mesh, this distance ensures that all nodes of degree 0 or 1 located on a same triangular face are connected.

The distance is offset by f to compensate the previous filtering task. Edge adding priority is given to the closer nodes. The task is completed when there is no more edge to add.

Lastly, the output graph is modified to bound the discretization of the edges. To this end, the longer edges are split into smaller edges of length d . For this, nodes are added on the relevant edges with a linear interpolation. Sub-edges are added between the consecutive points created and the initial edge is deleted. This ensures that no edge of the graph is longer than d . Then, the edges lower than $d/2$ are filtered (Fig. 7). This choice ensures to delete the edges of too little size and thus avoid the natural increase of the number of points per unit length of the later layers. The removal of over-discretized edges consists in scanning each node of the graph, and merging all the nodes directly connected to it that are located inside a sphere of radius $d/2$. The edges between merged nodes are deleted. The node kept during the merging process inherits of all the edges between the merged nodes and the other nodes of the graph. Thus, once longer edges are sub-discretized and over-discretized edges are removed, all edges lengths are bound between $d/2$ and $2*d$, with a major part of edges lengths close to d . Edges of length between d and $2*d$ are not sub-discretized to avoid over-discretization again.

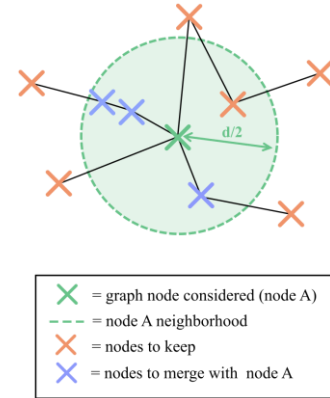


Fig. 7. Edges over-discretization removal.

4. Path simulations results

This section illustrates the paths generated with the algorithm whose main steps have been described in this paper. The input parameters values used during the simulations are detailed in Table 2.

Table 2. Simulations input parameters values

Input parameter (<i>unit</i>)	Value
h (mm)	2.0
d (mm)	0.5
f (mm)	0.5
e (mm)	1.0

The algorithm is first applied to the Schwarz P used to illustrate the method explanations of Section 3 (Fig. 8). Then, the algorithm is applied to the Schwarz G (Fig. 9) and the Neovius surface (Fig. 10) to show its versatility. In both cases, the substrate associated to the surface is a plane.

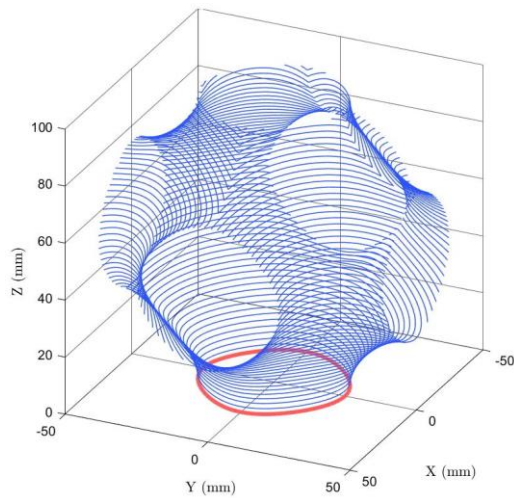


Fig. 8. Schwarz P ordered path (blue) from its initialization layer (red).

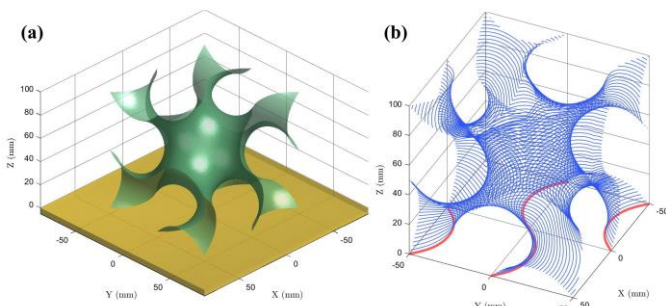


Fig. 9. (a) Schwarz G surface and substrate; (b) Schwarz G ordered path.

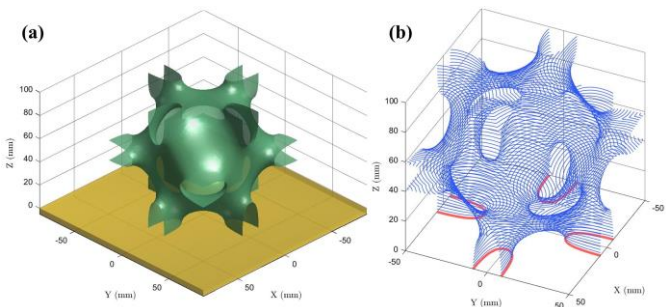


Fig. 10. (a) Neovius surface and substrate; (b) Neovius ordered path.

5. Conclusion and prospects

This paper describes the main steps of a numerical method to generate an organized path of any surface stored in facetized format for multi-axis DED additive manufacturing processes. The algorithm developed maximizes the layers length and meets the iso-Euclidean distance criterion between the tool and the workpiece during all the deposition process. First, the initial mesh is refined. Then, an initialization layer is computed as the intersection between the part to manufacture and the substrates

zones. Each new layer is determined from its previous layer. A set of subgraphs of the next layer is obtained by using triangle-sphere intersections, spherical linear interpolations and circle arcs merging. The subgraphs are then filtered and edges are added between the nodes to obtain the graph of the next layer. Edges are ordered to minimize the tool displacements. The method is suitable for high complexity surfaces and does not generate any support material to prevent parts inner areas inaccessibility for further surface machining.

However, tool-workpiece collisions were not considered during this study and have to be controlled for further manufacturing. A prioritizing of the regions of the surface to manufacture may lead to layers of different shape. This may avoid collisions to the cost of the maximization of layers length and an increase of the deposition starts and stops.

Acknowledgements

This work is supported by the French Agence Nationale de la Recherche (Paris, France) through the ANR BeShape Project [grant number ANR-18-CE10-0014-01].

References

- [1] D.-G. Ahn, « Directed energy deposition (DED) process: State of the art », *Int. J. Precis. Eng. Manuf.-Green Technol.*, vol. 8, n° 2, p. 703-742, 2021, doi: 10.1007/s40684-020-00302-7.
- [2] J. L. Prado-Cerqueira, J. L. Diéguez, et A. M. Camacho, « Preliminary development of a Wire and Arc Additive Manufacturing system (WAAM) », *Procedia Manuf.*, vol. 13, p. 895-902, 2017, doi: 10.1016/j.promfg.2017.09.154.
- [3] S. Restrepo, S. Ocampo, J. A. Ramírez, C. Paucar, et C. García, « Mechanical properties of ceramic structures based on triply periodic minimal surface (TPMS) processed by 3D printing », *J. Phys. Conf. Ser.*, vol. 935, n° 1, 2017, doi: 10.1088/1742-6596/935/1/012036.
- [4] V. Dhinakaran, J. Ajith, A. F. Y. Fahmidha, T. Jagadeesha, T. Sathish, et B. Stalin, « Wire Arc Additive Manufacturing (WAAM) process of nickel based superalloys—A review », *Mater. Today Proc.*, vol. 21, p. 920-925, 2020, doi: 10.1016/j.matpr.2019.08.159.
- [5] D. Ding, Z. Pan, D. Cuiuri, et H. Li, « Process planning for robotic wire and arc additive manufacturing », in *2015 IEEE 10th Conference on Industrial Electronics and Applications (ICIEA)*, 2015, p. 2000-2003. doi: doi.org/10.1109/iciea.2015.7334441.
- [6] D.-S. Shim, G.-Y. Baek, J.-S. Seo, G.-Y. Shin, K.-P. Kim, et K.-Y. Lee, « Effect of layer thickness setting on deposition characteristics in direct energy deposition (DED) process », *Opt. Laser Technol.*, vol. 86, p. 69-78, 2016, doi: 10.1016/j.optlastec.2016.07.001.
- [7] M. Chalvin, S. Campocasso, V. Hugel, et T. Baizeau, « Layer-by-layer generation of optimized joint trajectory for multi-axis robotized additive manufacturing of parts of revolution », *Robot. Comput.-Integr. Manuf.*, vol. 65, p. 101960, 2020, doi: 10.1016/j.procir.2019.02.017.
- [8] A. Diourté, F. Bugarin, C. Bordreuil, et S. Segonds, « Continuous three-dimensional path planning (CTPP) for complex thin parts with wire arc additive manufacturing », *Addit. Manuf.*, p. 101622, 2020, doi: 10.1016/j.addma.2020.101622.
- [9] K. Crane, C. Weischedel, et M. Wardetzky, « The heat method for distance computation », *Commun. ACM*, vol. 60, n° 11, p. 90-99, 2017, doi: 10.1145/3131280.
- [10] L. Yaxiong et Z. Yongchang, « A new algorithm for the directed Chinese postman problem », *Comput. Oper. Res.*, vol. 15, n° 6, p. 577-584, 1988, doi: 10.1016/0305-0548(88)90053-6.
- [11] V. Klee, « Maximal separation theorems for convex sets », *Trans. Am. Math. Soc.*, vol. 134, n° 1, p. 133-147, 1968, doi: doi.org/10.1090/s0002-9947-1968-0235457-9.
- [12] K. Shoemake, « Animating rotation with quaternion curves », in *Proceedings of the 12th annual conference on Computer graphics and interactive techniques*, 1985, p. 245-254. doi: 10.1145/325165.325242.